pubs.acs.org/acschemicalbiology

Article

Evaluation of the Cytosolic Uptake of HaloTag Using a pH-Sensitive Dye

JoLynn B. Giancola, Jonathan B. Grimm, Joomyung V. Jun, Yana D. Petri, Luke D. Lavis, and Ronald T. Raines*

Cite This: *ACS Chem. Biol.* 2024, 19, 908−915

Read Online

ACCESS | Metrics & More | Article Recommendations | Supporting Information

ABSTRACT: The efficient cytosolic delivery of proteins is critical for advancing novel therapeutic strategies. Current delivery methods are severely limited by endosomal entrapment, and detection methods lack sophistication in tracking the fate of delivered protein cargo. HaloTag, a commonly used protein in chemical biology and a challenging delivery target, is an exceptional model system for understanding and exploiting cellular delivery. Here, we employed a combinatorial strategy to direct HaloTag to the cytosol. We established the use of Virginia Orange, a pH-sensitive fluorophore, and Janelia Fluor 585, a similar but pH-agnostic fluorophore, in a fluorogenic assay to ascertain protein localization within human cells. Using this assay, we investigated HaloTag delivery upon modification with cell-penetrating peptides, carboxyl group esterification, and cotreatment with an endosomolytic agent. We found efficacious cytosolic entry with two distinct delivery methods. This study expands the toolkit for detecting the cytosolic access of proteins and highlights that multiple intracellular delivery strategies can be used synergistically to effect cytosolic access. Moreover, HaloTag is poised to serve as a platform for the delivery of varied cargo into human cells.

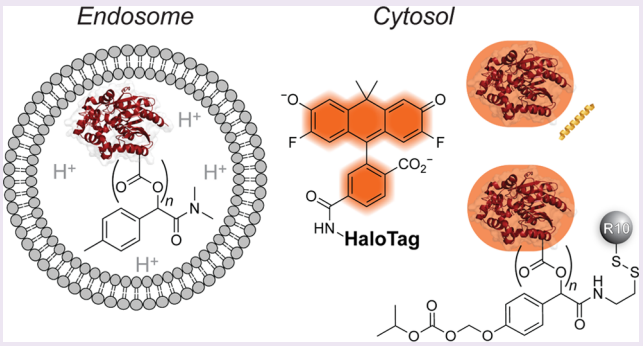

INTRODUCTION

Leveraging the remarkable potency and specificity of proteins has revolutionized the therapeutic landscape. Rationally designed biologics have shown efficacy in a wide range of etiologies, leading to their prevalence in the clinic.[1−3] To date, however, these advances have been restricted to extracellular targets, leaving an estimated 3/4 of disease-relevant, intracellular human proteins undruggable.[4] Unlike small-molecule therapeutics, which can enter cells via diffusion, proteins require adjuvants to mediate cellular uptake. Thus, the efficient intracellular delivery of proteins would both advance basic research and open new therapeutic avenues.

From this perspective, the HaloTag protein is an ideal candidate for investigating cytosolic delivery. HaloTag (HT7) is an engineered bacterial haloalkane dehalogenase, derived from *Rhodococcus* dehalogenase (DhaA), that has been altered[5] (L47V, S58T, D78G, Y87F, L88M, C128F, A155T, E160K, A167V, A172T, K175M, C176G, K195N, A224E, N227D, E257K, T264A, F272N, Y273L, P291S, A292T, Q294E, Q294E, Y295I, S^{296}, G^{297}) to prevent catalytic turnover but enable the *O*-alkylation of an active-site glutamic acid residue using a haloalkane of choice.[6] Depending on the substrate, the labeling kinetics of HaloTag are ∼10^4−10^7 M^{-1} s^{-1}, allowing for rapid saturation of the enzyme with a defined ligand.[7] Given its attractive features, HaloTag is frequently used for the imaging of fusion proteins, as a handle for protein purification, and as a model protein.[5,8−12]

The outer membrane of mammalian cells is highly anionic.[13−15] Because of repulsive Coulombic forces, HaloTag, which is a highly anionic protein (p*I* 4.9[16]), is a special challenge for cellular delivery (Figure S3).[17] Several approaches for cytosolic protein delivery have sought to overcome this barrier. Proteins have been translocated to the cytosol of cells via electroporation,[18] polymer encapsulation,[19] conjugation to transduction domains (e.g., cell-penetrating peptides),[4,20−23] supercharging,[24−27] cotreatment with endosomolytic agents,[28,29] thiol−disulfide exchange,[30] and cationic lipids.[31,32] Recently, several reversible methods have enabled the traceless delivery of proteins into cells,[33−36] thereby addressing an important consideration for clinical translation. The majority of the aforementioned strategies induce endosomal uptake of proteins, followed by endosomal escape to access the cytosol and the therapeutic target of interest.

Received: November 23, 2023
Revised: January 19, 2024
Accepted: February 13, 2024
Published: March 25, 2024

https://doi.org/10.1021/acschembio.3c00713
ACS Chem. Biol. 2024, 19, 908−915

Notably, endosomal escape is frequently a limiting factor in protein delivery experiments, as typically <10% of the cargo reaches the cytosol, and the remainder is trapped in the endosome and trafficked toward lysosomal degradation.[37]

Several functional assays have been developed to assess the fate of protein cargoes, including protein complementation assays,[38−40] corrective splicing assays,[41,42] and assays that leverage cytosolic enzymes to label an exogenously delivered tag.[43−47] In addition, fluorogenic assays[46] and fluorescence correlation spectroscopy[48−50] imaging techniques provide complementary approaches to assess protein internalization. Most of these methods, however, rely on enzymatic activity after "tag" recognition, which requires the engineering of new cell lines,[51] hampering generality. Alternative techniques require the use of highly specialized instrumentation and advanced modeling to yield experimental results.[51]

A pH-sensitive fluorophore could be the basis for a general strategy to discern the localization of the protein cargo. This approach would leverage the difference in pH between the cytosol, which has a near-neutral pH, and the endosome, which has an acidic pH of 5−6,[52,53] as "on" and "off" switches for fluorescence. Naphthofluorescein (ε = 44 000 M^{-1} cm^{-1}; Φ = 0.14),[54,55] in particular, has been used in this context.[56−59] Naphthofluorescein, however, contains an extensive aromatic ring system, which is disadvantageous given the propensity for cellular uptake and subsequent localization of small biomolecules to be altered by a pendant dye.[60−63] While the size of the fluorophore plays an outsized role in cell penetration of small biomolecules as compared to large ones, like HaloTag (~35 kDa), establishing a pH-based fluorescent reporter smaller than naphthofluorescein is desirable to minimize the effect of the tag in any biomolecule.

Simple substitutions within xanthene dyes enable the tuning of their spectroscopic properties.[64−73] For example, substitutions can bias the dye toward a closed lactone form, which has negligible fluorescence, or an open zwitterionic form, which is highly fluorescent. This equilibrium can also be affected by the microenvironment of the fluorophore.[74]

Two complementary carbaxanthene-based dyes are ideal for our purposes (Figure 1A). One is Janelia Fluor 585 (JF_{585}; ε_{max} = 156 000 M^{-1} cm^{-1}; Φ = 0.78), which is ~19-fold brighter than naphthofluorescein, has $\lambda_{max}/\lambda_{em}$ = 585/609 nm, is designed to fluoresce only after binding within the HaloTag active site, and does not have a proton that is titratable under physiological conditions.[67,69] The other dye is Virginia Orange (VO; ε = 90 900 M^{-1} cm^{-1}; Φ = 0.40), which is ~6-fold brighter than naphthofluorescein, has $\lambda_{max}/\lambda_{em}$ = 555/581 nm, and has highly pH-sensitive fluorescence (h = 1.46) with a transition at pH 6.75.[75,76] As early endosomes mature to late endosomes, their pH drops from ~6.5 to ~5.5.[77] Lysosomes, their ultimate locale, have pH ~4.5.[77] This acidity means that VO is virtually nonfluorescent in endosomes and lysosomes.[76] Hence, we hypothesized that the conjugation of JF_{585} or VO to HaloTag would enable the monitoring of its endosomal escape during protein delivery experiments and the quantification of the efficiency of its cytosolic entry (Figure 1B).

We investigated three distinct strategies for the cytosolic delivery of HaloTag(dye) constructs. Specifically, we explored conjugation with a cell-penetrating peptide, bioreversible esterification, and cotreatment with an endosomolytic agent to deliver HaloTag when conjugated to either JF_{585} or VO. We observed varying cellular localizations that depend upon the delivery strategy.

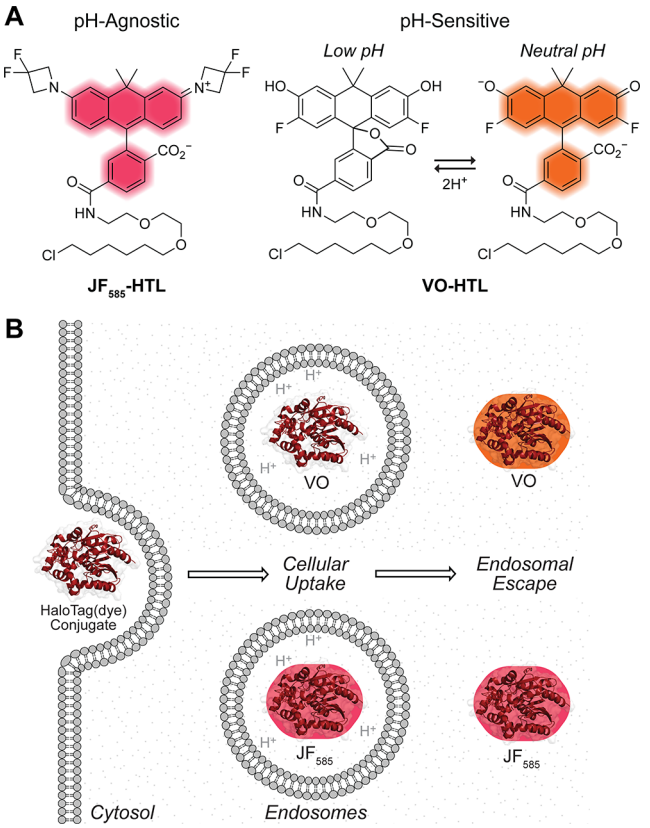

Figure 1. (A) Structures of JF_{585} and VO with a pendant HTL. (B) The low pH of endosomes and the pH-sensitive fluorescence of VO (but not JF_{585}) can be used to ascertain the subcellular localization of the HaloTag(dye) conjugates.

RESULTS

HaloTag(dye) Conjugates Can Inform Cellular Localization. Our first aim was to validate that JF_{585} and VO would be capable of distinguishing between endosomal and cytosolic compartments as a function of pH. We have reported the pH dependence of the fluorescence of JF_{585} and VO for the dyes alone[67,69,75,76] but not for HaloTag(dye) conjugates. To do so, we produced HaloTag in *Escherichia coli* with a TEV protease-cleavable polyhistidine tag for ease of purification. After purification and proteolytic cleavage (Figure S1), we conjugated HaloTag to either JF_{585} or VO equipped with a pendant HaloTag ligand (HTL) (Figure 1A). Analysis by mass spectrometry validated the identity of the HaloTag(JF_{585}) and HaloTag(VO) constructs (Figure S2). Next, we measured the fluorescence of each HaloTag(dye) as a function of pH. We found that the fluorescence of HaloTag(JF_{585}) is pH-agnostic (Figure 2A), as expected.[67,69] In contrast, we found that the fluorescence of HaloTag(VO) has a transition at pH 6.46 ± 0.01. This value is slightly lower than that of the dye alone (pH = 6.75),[75,76] which seems surprising given the anionic microenvironment that the dye occupies on the surface of HaloTag (Figures S3 and S4). However, the cooperativity of the pH transition is also smaller (h = 1.05) compared to that of the free dye (h = 1.46), suggesting stabilization of the open form of the dye by the polar environment of the protein surface and perhaps explaining the lower pK_a value. Taken together, this dye pair seems capable of distinguishing total protein uptake from that localized in the cytosol.

https://doi.org/10.1021/acschembio.3c00713
ACS Chem. Biol. 2024, 19, 908−915

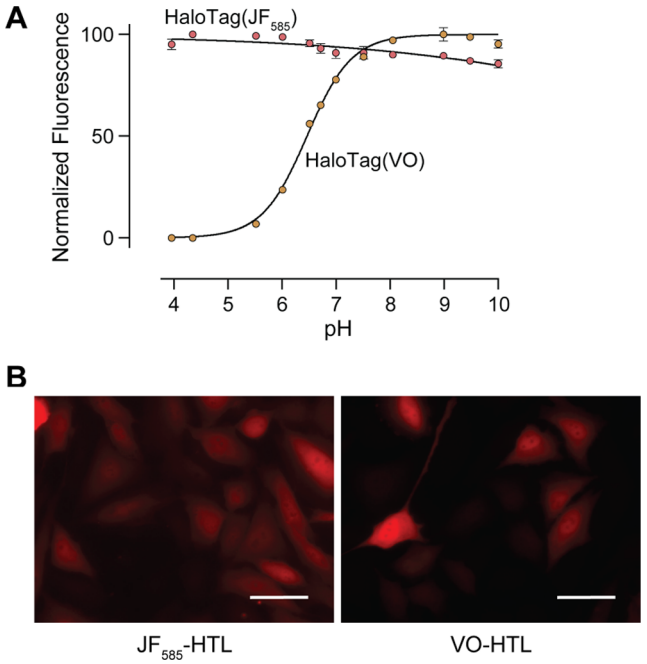

Figure 2. (A) pH dependence of the fluorescence of HaloTag(dye) constructs. Values are the mean ± SE (n = 3). HaloTag(VO) has an apparent pK_a of 6.46 ± 0.01 (h = 1.05). (B) Microscopy images of HeLa cells expressing cytosolically localized HaloTag and treated with either JF_{585}−HTL or VO−HTL. Images were normalized to untransfected cells treated with either fluorophore. Images are representative of uptake profiles of at least two independent experiments, each performed with three technical replicates. Scale bars: 50 μM. Additional images are shown in Figure S12.

To validate this difference in a cellular context, we used a transfection-based method to confirm the fluorescence of each dye in the cytosol. HeLa cells were transiently transfected with mRNA that encodes cytosolic HaloTag. Cells were then treated with JF_{585}−HTL or VO−HTL via pulse-chase epifluorescence imaging, followed by flow cytometry, to identify cells that express HaloTag (Figures 2B, S12−S14). We anticipated that when treated with either fluorescent ligand, cells containing HaloTag would fluoresce and that untransfected cells would not. Indeed, images of transfected cells treated with either fluorophore revealed a cytosolic HaloTag population, unlike images of untransfected cells. Additionally, we observed no background fluorescence in untransfected cells following the same treatment and washout period as transfected cells, indicating that the observed fluorescence signal was specifically associated with transfection (Figure S14). These data indicate that both dyes fluoresce when bound to HaloTag in the cytosol, enabling the unambiguous interpretation of protein delivery experiments.

Modification of HaloTag(dye) Conjugates. With a validated assay for cytosolic localization in hand, we sought to investigate the effect of different delivery agents on the uptake of HaloTag (Scheme 1). First, we appended deca-arginine (R10) to protein amino groups on each HaloTag-(dye) construct. To do so, we irreversibly modified HaloTag using lysine amidation with NHS-BCN. We then clicked an azide-containing R10 peptide onto the protein. The extent of labeling (typically, 0−1 R10 moieties) was determined by mass spectrometry (Figures S5 and S6).

Scheme 1. Semisynthesis of HaloTag(dye) Conjugates

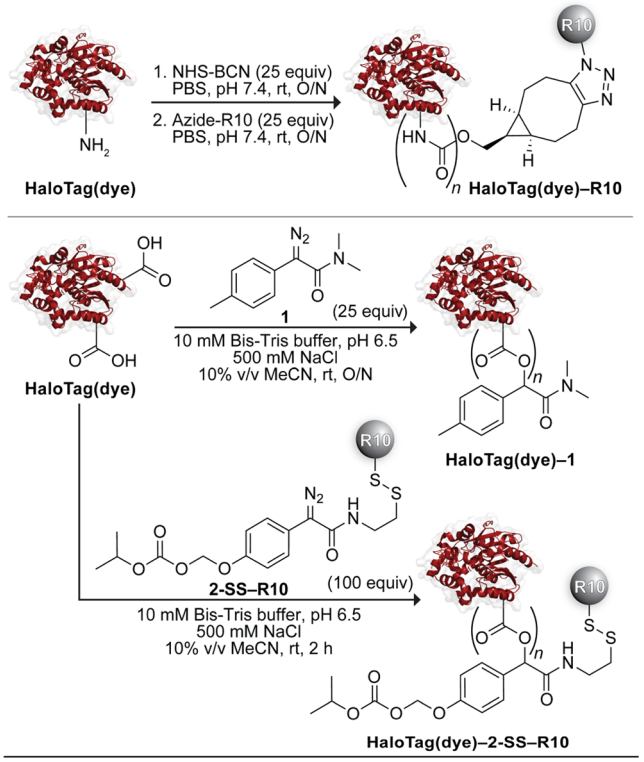

Next, we masked HaloTag carboxyl groups by esterification with a tuned diazo compound.[33,35] Upon cellular entry, endogenous intracellular esterases cleave these esters, unveiling the nascent protein. Previously, we reported that esterification using diazo compound **1** directed both the green fluorescent protein[33] and human ribonuclease 1[35] to the cytosol. Each of these proteins has, however, a pI value that is higher than that of HaloTag. To assess the cellular localization of HaloTag with diazo compound **1**, we modified the surface of HaloTag(JF_{585}) or HaloTag(VO) with this compound in an acidic buffer containing 500 mM NaCl to mediate labeling with minimal protein precipitation. We investigated two ranges of ester labels. The identity of the conjugates was confirmed using mass spectrometry and found to contain either 0−3 labels (low labeling) or 2−8 (high labeling) (Figures S7 and S8). Installation of more labels on the surface of HaloTag led to the precipitation of the protein, consistent with previous reports correlating the number of labels with protein insolubility as the pI of the protein approaches the pH of the solution.[78]

Recently, we deployed a novel diazo compound, **2**-SSpy, that enables a late-stage modification with a ligand of choice.[36] To modify HaloTag with this compound, **2**-SSpy was briefly premixed with the thiol-equipped R10 to form a disulfide linkage prior to reaction with the protein. The typical extent of labeling was found to be 0−1 (Figure S9). Based on a report of the solvent accessibility of cysteine residues in HaloTag,[79] we explored disulfide-linked HaloTag conjugates as another means for delivery but found the ensuing linkages to be unstable (Figure S11).

Finally, we used the L17E peptide in a cotreatment strategy to effect cellular entry. L17E is an engineered version of the toxic peptide M-lycotoxin from Wolf spider venom.[29] L17E was optimized to adopt an α-helical structure that selectively

https://doi.org/10.1021/acschembio.3c00713
ACS Chem. Biol. 2024, 19, 908−915

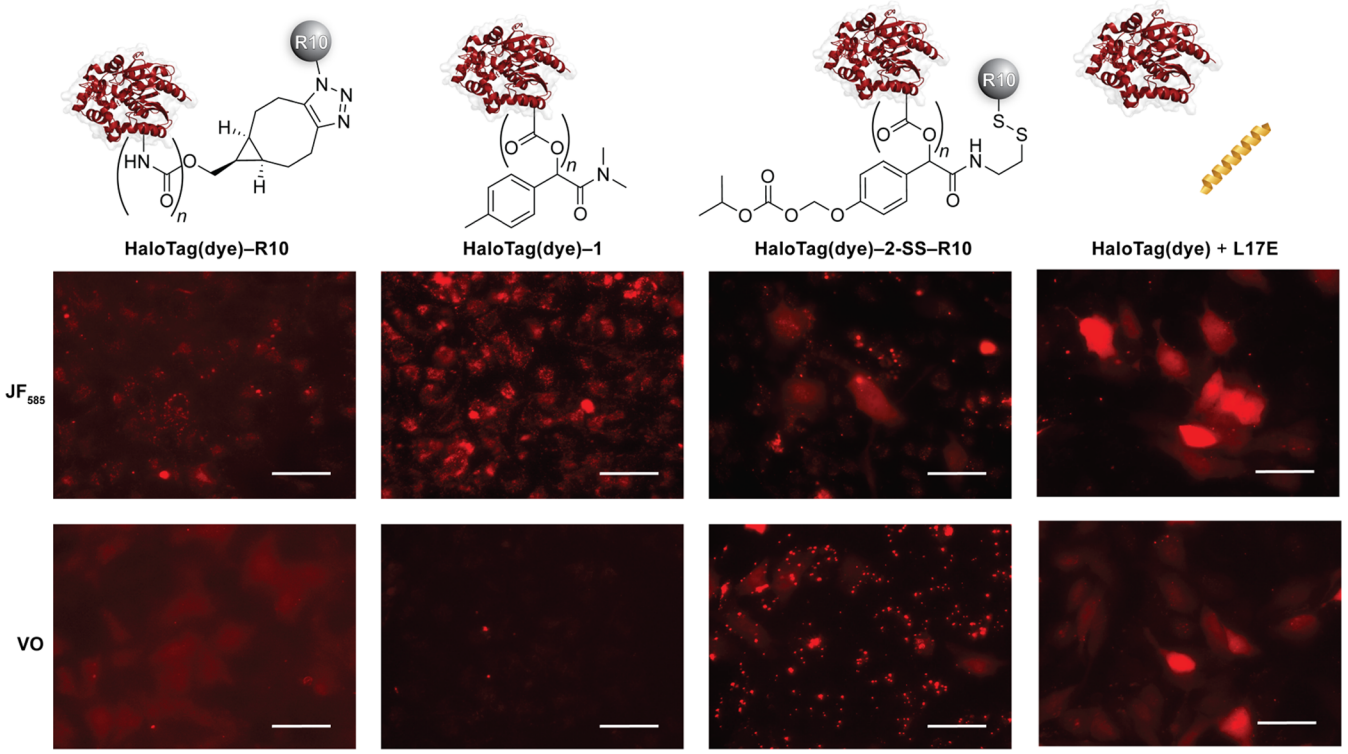

Figure 3. Microscopy images of HaloTag(dye) conjugates in HeLa cells normalized to cells treated with HaloTag(dye) only. For experimental conditions, see Table S1. Standardized laser intensities were normalized within each treatment condition. Images are representative of uptake profiles of at least two independent experiments performed with three technical replicates. Scale bars: 50 μM. Additional images are shown in Figures S15−S18.

disrupts endosomal membranes, thus mediating endosomal escape of the cotreated protein or other cargo into the cytosol. Altogether, we evaluated four distinct uptake strategies using the complementary dye pair.

Cellular Uptake Experiments with Microscopy. We next assessed the uptake profiles of the protein constructs in live HeLa cells. Cells were treated in serum-free DMEM medium at concentrations and times that were optimized for each HaloTag(JF_{585}) conjugate (Table S1). Subsequent paired experiments were conducted side-by-side with HaloTag(JF_{585}) and HaloTag(VO) conjugates. Epifluorescence microscopy was used to assess cellular localization. We found that all bioconjugates were taken up by cells, with differences in cytosolic access based on the delivery method (Figure 3).

HaloTag(dye)−R10. HaloTag(JF_{585})−R10 demonstrated exclusively punctate staining, indicative of endosomal entrapment (Figure 3). When taken together with HaloTag(VO)−R10, however, we observed low fluorescence staining of the cytosol, indicative of a small degree of endosomal escape. Given the anionic nature of the HaloTag surface (Figure S3), we were not surprised to find that a cationic cell-penetrating peptide does not mediate robust cellular entry.

HaloTag(dye)−1. Surface esterification with diazo compound **1** was used to investigate the effect of the extent of labeling on HaloTag uptake. We observed successful cellular uptake but only with a high level of esterification. Imaging revealed endosomal entrapment, evidenced by punctate staining in cells treated with HaloTag(JF_{585})−**1** and the absence of signal in cells treated with HaloTag(VO)−**1** (Figure 3). We attribute the endosomal entrapment of esterified HaloTag to the high anionicity of HaloTag. This anionicity cannot be overcome by esterification with diazo compound **1**, which ultimately serves to increase the hydrophobicity while only modestly decreasing the anionicity of the protein surface. We did not observe any cellular uptake with a low level of esterification (Figures S20 and S21).

HaloTag(dye)−2-SS−R10. HeLa cells treated with a **2**-SS−R10 ester conjugate showed mixed intracellular localization (Figure 3). Many clusters of cells exhibited cytosolic localization, with diffuse intracellular staining throughout the entire compartment. When cells treated with HaloTag(JF_{585})−**2**-SS−R10 were imaged at a higher laser intensity, punctate staining could be observed that was absent in cells treated with HaloTag(VO)−**2**-SS−R10, indicating endosomal entrapment. We also noted evidence of protein aggregation on the surface of cells treated with HaloTag(VO)−**2**-SS−R10, which was not observed under other treatment conditions. Nonetheless, the combination of a cell-penetrating peptide with esterification yielded cytosolic access.

HaloTag(dye) Plus L17E. Finally, we cotreated HeLa cells with HaloTag(dye) constructs + L17E. Fluorescence microscopy showed that both constructs localized robustly in the cytosol of cells, especially concentrated in clusters, as evidenced by diffuse staining throughout the cytosol and nucleus (Figure 3). With HaloTag(JF_{585}), we did not observe punctate staining indicative of endosomal entrapment. Although L17E has been used with other proteins and biomolecules,[29,80−83] the demonstration of its efficacy in delivering highly anionic protein cargo is, to our knowledge, unprecedented.

Cellular Uptake Experiments with Flow Cytometry. An advantage of the JF_{585}/VO dye pair is its ability to differentiate between bulk cellular uptake and cytosolic localization of conjugates. Having observed uptake patterns

https://doi.org/10.1021/acschembio.3c00713
ACS Chem. Biol. 2024, 19, 908−915

that varied between conjugates with fluorescence microscopy, we used flow cytometry to assess delivery efficiencies, which describe the relationship between the total amount of protein cargo taken up by the cell and the amount that ultimately reaches the cytosol. Because of the heterogeneity between each batch of prepared conjugates, as a result of stochastic surface labeling, we sought an analysis that would provide meaningful comparisons. Accordingly, we established a workflow, in which cells were first imaged via microscopy and then analyzed by flow cytometry.

Gratifyingly, the flow cytometry results were in agreement with the cellular uptake observed with microscopy. In cells treated with HaloTag(dye)−R10, we observed a modest shift in the bulk population, demonstrating a low level of endosomal escape (Figures S22 and S23). When modified with 2−8 ester labels, HaloTag(dye)−**1** was efficiently taken up into endosomes but did not exhibit the VO signal that would have been indicative of endosomal escape (Figure S24). By contrast, microscopy revealed a subset of cells cotreated with HaloTag(dye) and L17E exhibited high cellular uptake with both dyes and the absence of punctate staining with HaloTag(JF_{585}), indicating highly efficient cytosolic entry. Consistent with the robust cytosolic delivery of HaloTag(dye) in the presence of L17E that we observed via microscopy, we also observed a subset of highly fluorescent cells and little change in the bulk population via flow cytometry (Figure S25). The percent of cells in each sample treated with HaloTag(dye) + L17E were the same, reinforcing the high efficiency of cytosolic entry. Although we observed the cellular uptake and cytosolic entry of HaloTag(dye)−**2**-SS−R10 conjugates with both fluorophores via microscopy, the VO conjugate formed aggregates or coacervates on the surface of cells that were resistant to removal by washing and precluded analysis by flow cytometry (Figure S17).

From our flow cytometry analysis, we calculated the mean fluorescence intensity (MFI) of cells treated with HaloTag(dye) conjugates (Figure 4). When cells were treated with HaloTag(JF_{585}) conjugates, we observed MFI values of 1138, 3354, and 396 AU for HaloTag(JF_{585})−R10, HaloTag(JF_{585})−**1**, and HaloTag(JF_{585}) + L17E, respectively. These values highlight that HaloTag(JF_{585})−**1** is ∼3-fold more effective at being taken up by cells than HaloTag(JF_{585})−R10 and that HaloTag(JF_{585}) + L17E is only ∼1/3 as effective at enabling cellular uptake when compared to HaloTag(JF_{585})−R10. Yet, when cells were treated with HaloTag(VO) conjugates, we observed MFI values of 328, −80, and 591 AU for HaloTag(VO)−R10, HaloTag(VO)−**1**, and HaloTag(VO) + L17E, respectively. This demonstrates that HaloTag(VO) + L17E is ∼2-fold more effective at cytosolic delivery than HaloTag(VO)−R10 and that HaloTag(VO)−**1** is not detected in the cytosol of cells. These data are summarized in Table 1.

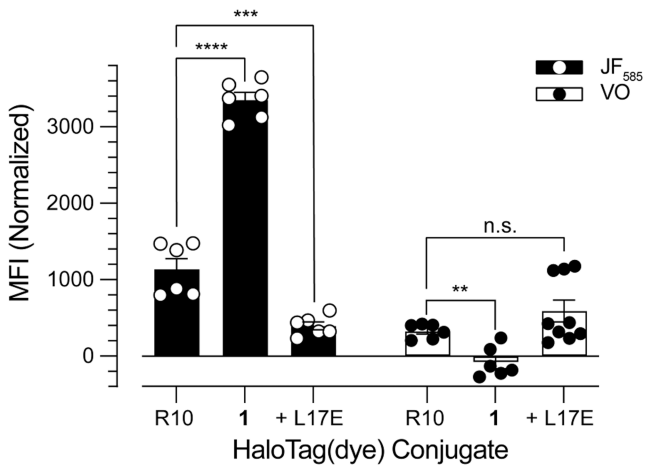

Figure 4. Mean fluorescence intensity (MFI) of HaloTag(dye) conjugates in HeLa cells. For experimental conditions, see Table S1. Values are the mean ± SE from at least two independent experiments, each performed with three technical replicates; ****$p < 0.0001$, ***$p < 0.0005$, **$p < 0.0011$. The average fluorescence background, calculated from cells treated with HaloTag(dye) alone, was subtracted from all of the treatment conditions. Standardized laser intensities were used for all experiments.

Table 1. Summary of Cellular Delivery Efficiencies

delivery strategy	total cellular uptake (MFI^{JF585})[a]	cytosolic delivery (MFI^{VO})[a]	delivery efficiency (γ)[a]
R10	1.0	1.0	1.0
1	3.0	0.0	0.0
L17E	0.35	1.8	5.2

[a]Values are normalized to the uptake profiles of HaloTag(dye)−R10, which is defined as 1.0. MFI^{JF585} and MFI^{VO} represent the ratio of the MFI of each delivery strategy to the MFI of R10.

With flow cytometry data sets in hand, we calculated the delivery efficiency (γ) by using an equation[56] that deploys the MFI of the JF_{585} and VO conjugates:

$$\gamma = \left(\frac{MFI^{VO}_{vehicle}}{MFI^{JF_{585}}_{vehicle}}\right) \Big/ \left(\frac{MFI^{VO}_{R10}}{MFI^{JF_{585}}_{R10}}\right) \quad (1)$$

Equation 1 relates the total cellular uptake (JF_{585}) and the cytosolic uptake (VO) of a given delivery strategy (denoted as "vehicle") to one defined as a reference. This normalization ultimately quantifies the efficiency of cytosolic delivery as a fold-change compared to the reference. Because R10 is a well-known cell-penetrating peptide, we set HaloTag(dye)−R10 as our reference and normalized other delivery strategies to that conjugate (Table 1).

Our analysis reveals that while the esterification of HaloTag(dye) with diazo compound **1** provides highly effective entrance into cells via endocytosis, this modification does not afford cytosolic access. This underscores the idiosyncratic nature of protein delivery into cells and highlights the challenge of providing cytosolic access to an extremely anionic payload like HaloTag. In contrast, we observed that the endosomolytic peptide L17E is less efficient at providing cellular entry than R10, but the fraction of HaloTag that reaches the cytosol is ∼2-fold greater than that of R10, representing an ∼5-fold increase in delivery efficiency. Thus, L17E is highly efficient at circumventing endosomal entrapment and lysosomal degradation and, ultimately, delivering HaloTag to the cytosol.

CONCLUSIONS

Current methods to assess the cytosolic delivery of proteins are time-consuming to establish, require specialized instrumentation, or introduce enzymatic "tag" recognition sequences that limit generality. Herein, we describe a dye pair with the ability to assess protein delivery efficiencies, enabling a nuanced understanding of how protein delivery agents affect cellular

https://doi.org/10.1021/acschembio.3c00713
ACS Chem. Biol. 2024, 19, 908−915

uptake and cytosolic access. Using this novel method, we report the unprecedented (to our knowledge) delivery of HaloTag, a highly anionic and thus challenging protein target, to the cytosol of mammalian cells. We anticipate that our results will facilitate the further development of HaloTag as a useful cellular delivery platform to mediate the delivery of other proteins and payloads.

■ ASSOCIATED CONTENT

Supporting Information

The Supporting Information is available free of charge at https://pubs.acs.org/doi/10.1021/acschembio.3c00713.

Experimental procedures; Table S1; Figures S1−S25; and compound characterization (PDF)

■ AUTHOR INFORMATION

Corresponding Author

Ronald T. Raines − *Department of Chemistry, Massachusetts Institute of Technology, Cambridge, Massachusetts 02139, United States;* orcid.org/0000-0001-7164-1719; Email: rtraines@mit.edu

Authors

JoLynn B. Giancola − *Department of Chemistry, Massachusetts Institute of Technology, Cambridge, Massachusetts 02139, United States*

Jonathan B. Grimm − *Janelia Research Campus, Howard Hughes Medical Institute, Ashburn, Virginia 20147, United States;* orcid.org/0000-0003-0331-4200

Joomyung V. Jun − *Department of Chemistry, Massachusetts Institute of Technology, Cambridge, Massachusetts 02139, United States;* orcid.org/0000-0002-7276-4806

Yana D. Petri − *Department of Chemistry, Massachusetts Institute of Technology, Cambridge, Massachusetts 02139, United States;* orcid.org/0000-0001-6064-7971

Luke D. Lavis − *Janelia Research Campus, Howard Hughes Medical Institute, Ashburn, Virginia 20147, United States;* orcid.org/0000-0002-0789-6343

Complete contact information is available at: https://pubs.acs.org/10.1021/acschembio.3c00713

Funding

J.V.J. was supported by a Life Sciences Research Foundation fellowship sponsored by the Shurl and Kay Curci Foundation. Y.D.P. was supported by NSF Graduate Research Fellowship 4000143422. This work was supported by Grant R35 GM148220 (NIH) and the Howard Hughes Medical Institute (HHMI).

Notes

The authors declare no competing financial interest.

■ ACKNOWLEDGMENTS

The authors are grateful to J. Yang, E. C. Wralstad, N. S. Abularrage, R. L. McPherson, and S. D. Brucks for helpful scientific discussions and to R. L. McPherson, S. D. Brucks, V. M. Marando, M. C. Hoffman, and K. J. Hetrick for their assistance in reviewing the manuscript. They are grateful to the Koch Institute High Throughput Facilities Core for providing the HeLa cell line and for performing mycoplasma testing.

■ REFERENCES

(1) Deshaies, R. J. Multispecific drugs herald a new era of biopharmaceutical innovation. *Nature* **2020**, *580*, 329−338.

(2) Urquhart, L. Top product forecasts for 2021. *Nat. Rev. Drug Discovery* **2021**, *20*, 10.

(3) Urquhart, L. Top product forecasts for 2022. *Nat. Rev. Drug Discovery* **2022**, *21*, 11.

(4) Dougherty, P. G.; Sahni, A.; Pei, D. Understanding cell penetration of cyclic peptides. *Chem. Rev.* **2019**, *119*, 10241−10287.

(5) Los, G. V.; Encell, L. P.; McDougall, M. G.; Hartzell, D. D.; Karassina, N.; Zimprich, C.; Wood, M. G.; Learish, R.; Ohana, R. F.; Urh, M.; Simpson, D.; Mendez, J.; Zimmerman, K.; Otto, P.; Vidugiris, G.; Zhu, J.; Darzins, A.; Klaubert, D. H.; Bulleit, R. F.; Wood, K. V. HaloTag: A novel protein labeling technology for cell imaging and protein analysis. *ACS Chem. Biol.* **2008**, *3*, 373−382.

(6) Encell, L. P.; Ohana, R. F.; Zimmerman, K.; Otto, P.; Vidugiris, G.; Wood, M. G.; Los, G. V.; McDougall, M. G.; Zimprich, C.; Karassina, N.; Learish, R. D.; Hurst, R.; Hartnett, J.; Wheeler, S.; Stecha, P.; English, J.; Zhao, K.; Mendez, J.; Benink, H. A.; Murphy, N.; Daniels, D. L.; Slater, M. R.; Urh, M.; Darzins, A.; Klaubert, D. H.; Bulleit, R. F.; Wood, K. V. Suppl 1: Development of a dehalogenase-based protein fusion tag capable of rapid, selective and covalent attachment to customizable ligands. *Curr. Chem. Genomics* **2013**, *6*, 55−71.

(7) Wilhelm, J.; Kühn, S.; Tarnawski, M.; Gotthard, G.; Tünnermann, J.; Tänzer, T.; Karpenko, J.; Mertes, N.; Xue, L.; Uhrig, U.; Reinstein, J.; Hiblot, J.; Johnsson, K. Kinetic and structural characterization of the self-labeling protein tags HaloTag7, SNAP-tag, and CLIP-tag. *Biochemistry* **2021**, *60*, 2560−2575.

(8) England, C. G.; Luo, H.; Cai, W. HaloTag technology: A versatile platform for biomedical applications. *Bioconjugate Chem.* **2015**, *26*, 975−986.

(9) Buckley, D. L.; Raina, K.; Darricarrere, N.; Hines, J.; Gustafson, J. L.; Smith, I. E.; Miah, A. H.; Harling, J. D.; Crews, C. M. HaloPROTACS: Use of small molecule PROTACs to induce degradation of HaloTag fusion proteins. *ACS Chem. Biol.* **2015**, *10*, 1831−1837.

(10) Erdmann, R. S.; Baguley, S. W.; Richens, J. H.; Wissner, R. F.; Xi, Z.; Allgeyer, E. S.; Zhong, S.; Thompson, A. D.; Lowe, N.; Butler, R.; Bewersdorf, J.; Rothman, J. E.; St Johnston, D.; Schepartz, A.; Toomre, D. Labeling strategies matter for super-resolution microscopy: A comparison between HaloTags and SNAP-tags. *Cell Chem. Biol.* **2019**, *26*, 584−592.

(11) Straková, K.; Lopez-Andarias, J.; Jimenez-Rojo, N.; Chambers, J. E.; Marciniak, S. J.; Riezman, H.; Sakai, N.; Matile, S. Haloflippers: A general tool for the fluorescence imaging of precisely localized membrane tension changes in living cells. *ACS Cent. Sci.* **2020**, *6*, 1376−1385.

(12) Chen, W.; Younis, M. H.; Zhao, Z.; Cai, W. Recent biomedical advances enabled by HaloTag technology. *Biocell* **2022**, *46*, 1789 DOI: 10.32604/biocell.2022.018197.

(13) Coulomb, C. A. *Collection de Mémoires Relatifs a la Physique*; Gauthier−Villars: Paris, 1884.

(14) Gillmor, C. S. *Coulomb and the Evolution of Physics and Engineering in Eighteenth-Century France*; Princeton University Press: Princeton, NJ, 1971.

(15) Varki, A.; Cummings, R. D.; Esko, J. D.; Freeze, H. H.; Stanley, P.; Bertozzi, C. R.; Hart, G. W.; Etzler, M. E. *Essentials of Glycobiology*; Cold Spring Harbor Laboratory Press: Cold Spring Harbor, NY, 2009.

(16) Gasteiger, E.; Hoogland, C.; Gattiker, A.; Duvaud, S.; Wilkins, M. R.; Appel, R. D.; Bairoch, A. Protein Identification and Analysis Tools on the ExPASy Server. In *The Proteomics Protocols Handbook*; Walker, J. M., Ed.; Humana Press: Totowa, NJ, 2005; pp 571−607.

(17) Palte, M. J.; Raines, R. T. Interaction of nucleic acids with the glycocalyx. *J. Am. Chem. Soc.* **2012**, *134*, 6218−6223.

(18) Kim, S.; Kim, D.; Cho, S. W.; Kim, J.; Kim, J. S. Highly efficient RNA-guided genome editing in human cells via delivery of purified Cas9 ribonucleoproteins. *Genome Res.* **2014**, *24*, 1012−1019.

(19) Lee, Y.-W.; Luther, D. C.; Goswami, R.; Jeon, T.; Clark, V.; Elia, J.; Gopalakrishnan, S.; Rotello, V. M. Direct cytosolic delivery of proteins through coengineering of proteins and polymeric delivery vehicles. *J. Am. Chem. Soc.* **2020**, *142*, 4349−4355.
(20) Schwarze, S. R.; Ho, A.; Vocero-Akbani, A.; Dowdy, S. F. In vivo protein transduction: Delivery of a biologically active protein into the mouse. *Science* **1999**, *285*, 1569−1572.
(21) Nagel, Y. A.; Raschle, P. S.; Wennemers, H. Effect of preorganized charge-display on the cell-penetrating properties of cationic peptides. *Angew. Chem., Int. Ed.* **2017**, *56*, 122−126.
(22) Schneider, A. F. L.; Kithil, M.; Cardoso, M. C.; Lehmann, M.; Hackenberger, C. P. R. Cellular uptake of large biomolecules enabled by cell-surface-reactive cell-penetrating peptide additives. *Nat. Chem.* **2021**, *13*, 530−539.
(23) Zhang, X.; Cattoglio, C.; Zoltek, M.; Vetralla, C.; Mozumdar, D.; Schepartz, A. Dose-dependent nuclear delivery and transcriptional repression with a cell-penetrant MeCP2. *ACS Cent. Sci.* **2023**, *9*, 277−288.
(24) Fuchs, S. M.; Raines, R. T. Arginine grafting to endow cell permeability. *ACS Chem. Biol.* **2007**, *2*, 167−170.
(25) Fuchs, S. M.; Rutkoski, T. J.; Kung, V. M.; Groeschl, R. T.; Raines, R. T. Increasing the potency of a cytotoxin with an arginine graft. *Protein Eng., Des. Sel.* **2007**, *20*, 505−509, DOI: 10.1093/protein/gzm051.
(26) McNaughton, B. R.; Cronican, J. J.; Thompson, D. B.; Liu, D. R. Mammalian cell penetration, siRNA transfection, and DNA transfection by supercharged proteins. *Proc. Natl. Acad. Sci. U.S.A.* **2009**, *106*, 6111−6116.
(27) Thompson, D. B.; Cronican, J. J.; Liu, D. R. Engineering and identifying supercharged proteins for macromolecule delivery into mammalian cells. *Methods Enzymol.* **2012**, *503*, 293−319.
(28) Li, W.; Nicol, F.; Szoka, F. C., Jr. GALA: A designed synthetic pH-responsive amphipathic peptide with applications in drug and gene delivery. *Adv. Drug Del. Rev.* **2004**, *56* (7), 967−985, DOI: 10.1016/j.addr.2003.10.041.
(29) Akishiba, M.; Takeuchi, T.; Kawaguchi, Y.; Sakamoto, K.; Yu, H. H.; Nakase, I.; Takatani-Nakase, T.; Madani, F.; Gräslund, A.; Futaki, S. Cytosolic antibody delivery by lipid-sensitive endosomolytic peptide. *Nat. Chem.* **2017**, *9*, 751−761.
(30) Laurent, Q.; Martinent, R.; Moreau, D.; Winssinger, N.; Sakai, N.; Matile, S. Oligonucleotide phosphorothioates enter cells by thiol-mediated uptake. *Angew. Chem., Int. Ed.* **2021**, *60*, 19102−19106.
(31) Futaki, S.; Ohashi, W.; Suzuki, T.; Niwa, M.; Tanaka, S.; Ueda, K.; Harashima, H.; Sugiura, Y. Stearylated arginine-rich peptides: A new class of transfection systems. *Bioconjugate Chem.* **2001**, *12*, 1005−1011.
(32) Sakamoto, K.; Michibata, J.; Hirai, Y.; Ide, A.; Ikitoh, A.; Takatani-Nakase, T.; Futaki, S. Potentiating the membrane interaction of an attenuated cationic amphiphilic lytic peptide for intracellular protein delivery by anchoring with pyrene moiety. *Bioconjugate Chem.* **2021**, *32*, 950−957.
(33) Mix, K. A.; Lomax, J. E.; Raines, R. T. Cytosolic delivery of proteins by bioreversible esterification. *J. Am. Chem. Soc.* **2017**, *139*, 14396−14398.
(34) Schneider, A. F. L.; Wallabregue, A. L. D.; Franz, L.; Hackenberger, C. P. R. Targeted subcellular protein delivery using cleavable cyclic cell-penetrating peptides. *Bioconjugate Chem.* **2019**, *30*, 400−404.
(35) Ressler, V. T.; Mix, K. A.; Raines, R. T. Esterification delivers a functional enzyme into a human cell. *ACS Chem. Biol.* **2019**, *14*, 599−602.
(36) Jun, J. V.; Petri, Y. D.; Erickson, L. W.; Raines, R. T. Modular diazo compound for the bioreversible late-stage modification of proteins. *J. Am. Chem. Soc.* **2023**, *145*, 6615−6621.
(37) Chao, T.-Y.; Raines, R. T. Fluorogenic label to quantify the cytosolic delivery of macromolecules. *Mol. Biosyst.* **2013**, *9*, 339−342.
(38) Johnsson, N.; Varshavsky, A. Split ubiquitin as a sensor of protein interactions in vivo. *Proc. Natl. Acad. Sci. U.S.A.* **1994**, *91*, 10340−10344.
(39) Cabantous, S.; Terwilliger, T. C.; Waldo, G. S. Protein tagging and detection with engineered self-assembling fragments of green fluorescent protein. *Nat. Biotechnol.* **2005**, *23*, 102−107.
(40) Kato, N.; Jones, J. The split luciferase complementation assay. *Methods Mol. Biol.* **2010**, *655*, 359−376.
(41) Dominski, Z.; Kole, R. Restoration of correct splicing in thalassemic pre-mRNA by antisense oligonucleotides. *Proc. Natl. Acad. Sci. U.S.A.* **1993**, *90*, 8673−8677.
(42) Kang, S. H.; Cho, M. J.; Kole, R. Up-regulation of luciferase gene expression with antisense oligonucleotides: Implications and applications in functional assay development. *Biochemistry* **1998**, *37*, 6235−6239.
(43) Loison, F.; Nizard, P.; Sourisseau, T.; Le Goff, P.; Debure, L.; Le Drean, Y.; Michel, D. A ubiquitin-based assay for the cytosolic uptake of protein transduction domains. *Mol. Ther.* **2005**, *11*, 205−214.
(44) Stanford, S. M.; Krishnamurthy, D.; Kulkarni, R. A.; Karver, C. E.; Bruenger, E.; Walker, L. M.; Ma, C. T.; Chung, T. D. Y.; Sergienko, E.; Bottini, N.; Barrios, A. M. PCAP-based peptide substrates: The new tool in the box of tyrosine phosphatase assays. *Methods* **2014**, *65*, 165−174.
(45) Verdurmen, W. P. R.; Luginbühl, M.; Honegger, A.; Plückthun, A. Efficient cell-specific uptake of binding proteins into the cytoplasm through engineered modular transport systems. *J. Controlled Release* **2015**, *200*, 13−22.
(46) Chyan, W.; Raines, R. T. Enzyme-activated fluorogenic probes for live-cell and in vivo imaging. *ACS Chem. Biol.* **2018**, *13*, 1810−1823.
(47) Peraro, L.; Deprey, K. L.; Moser, M. K.; Zou, Z.; Ball, H. L.; Levine, B.; Kritzer, J. A. Cell penetration profiling using the chloroalkane penetration assay. *J. Am. Chem. Soc.* **2018**, *140*, 11360−11369.
(48) Larochelle, J. R.; Cobb, G. B.; Steinauer, A.; Rhoades, E.; Schepartz, A. Fluorescence correlation spectroscopy reveals highly efficient cytosolic delivery of certain penta-arg proteins and stapled peptides. *J. Am. Chem. Soc.* **2015**, *137*, 2536−2541.
(49) Illien, F.; Rodriguez, N.; Amoura, M.; Joliot, A.; Pallerla, M.; Cribier, S.; Burlina, F.; Sagan, S. Quantitative fluorescence spectroscopy and flow cytometry analyses of cell-penetrating peptides internalization pathways: Optimization, pitfalls, comparison with mass spectrometry quantification. *Sci. Rep.* **2016**, *6*, 36938 DOI: 10.1038/srep36938.
(50) Rezgui, R.; Blumer, K.; Yeoh-Tan, G.; Trexler, A. J.; Magzoub, M. Precise quantification of cellular uptake of cell-penetrating peptides using fluorescence-activated cell sorting and fluorescence correlation spectroscopy. *Biochim. Biophys. Acta, Biomembr.* **2016**, *1858*, 1499−1506, DOI: 10.1016/j.bbamem.2016.03.023.
(51) Deprey, K.; Becker, L.; Kritzer, J.; Plückthun, A. Trapped! A critical evaluation of methods for measuring total cellular uptake versus cytosolic localization. *Bioconjugate Chem.* **2019**, *30*, 1006−1027.
(52) Tycko, B.; Keith, C. H.; Maxfield, F. R. Rapid acidification of endocytic vesicles containing asialoglycoprotein in cells of a human hepatoma line. *J. Cell Biol.* **1983**, *97*, 1762−1776.
(53) Murphy, R. F.; Powers, S.; Cantor, C. R. Endosome pH measured in single cells by dual fluorescence flow cytometry: Rapid acidification of insulin to pH 6. *J. Cell Biol.* **1984**, *98*, 1757−1762.
(54) Lee, L. G.; Berry, G. M.; Chen, C.-H. Vita Blue: A new 633-nm excitable fluorescent dye for cell analysis. *Cytometry* **1989**, *10*, 151−164.
(55) Wainwright, M. The use of dyes in modern biomedicine. *Biotechnol. Histochem.* **2003**, *78*, 147−155.
(56) Qian, Z.; Dougherty, P. G.; Pei, D. Monitoring the cytosolic entry of cell-penetrating peptides using a pH-sensitive fluorophore. *Chem. Commun.* **2015**, *51*, 2162−2165.
(57) Qian, Z.; Martyna, A.; Hard, R. L.; Wang, J.; Appiah-Kubi, G.; Coss, C.; Phelps, M. A.; Rossman, J. S.; Pei, D. Discovery and mechanism of highly efficient cyclic cell-penetrating peptides. *Biochemistry* **2016**, *55*, 2601−2612.

(58) Stolle, A. S.; Norkowski, S.; Körner, B.; Schmitz, J.; Lüken, L.; Frankenberg, M.; Rüter, C.; Schmidt, M. A. T3SS-independent uptake of the short-trip toxin-related recombinant NleC effector of enteropathogenic *Escherichia coli* leads to NF-κB p65 cleavage. *Front. Cell. Infect. Microbiol.* **2017**, *7*, 119.
(59) Chen, K.; Pei, D. Engineering cell-permeable proteins through insertion of cell-penetrating motifs into surface loops. *ACS Chem. Biol.* **2020**, *15*, 2568−2576.
(60) Fischer, R.; Waizenegger, T.; Köhler, K.; Brock, R. A quantitative validation of fluorophore-labelled cell-permeable peptide conjugates: Fluorophore and cargo dependence of import. *Biochim. Biophys. Acta, Biomembr.* **2002**, *1564*, 365−374, DOI: 10.1016/S0005-2736(02)00471-6.
(61) Puckett, C. A.; Barton, J. K. Fluorescein redirects a ruthenium-octaarginine conjugate to the nucleus. *J. Am. Chem. Soc.* **2009**, *131*, 8738−8739.
(62) Walrant, A.; Matheron, L.; Cribier, S.; Chaignepain, S.; Jobin, M. L.; Sagan, S.; Alves, I. D. Direct translocation of cell-penetrating peptides in liposomes: A combined mass spectrometry quantification and fluorescence detection study. *Anal. Biochem.* **2013**, *438*, 1−10.
(63) Birch, D.; Christensen, M. V.; Staerk, D.; Franzyk, H.; Nielsen, H. M. Fluorophore labeling of a cell-penetrating peptide induces differential effects on its cellular distribution and affects cell viability. *Biochim. Biophys. Acta, Biomembr.* **2017**, *1859*, 2483−2494, DOI: 10.1016/j.bbamem.2017.09.015.
(64) Lavis, L. D.; Raines, R. T. Bright ideas for chemical biology. *ACS Chem. Biol.* **2008**, *3*, 142−155.
(65) Grimm, J. B.; Sung, A. J.; Legant, W. R.; Hulamm, P.; Matlosz, S. M.; Betzig, E.; Lavis, L. D. Carbofluoresceins and carborhodamines as scaffolds for high-contrast fluorogenic probes. *ACS Chem. Biol.* **2013**, *8*, 1303−1310.
(66) Lavis, L. D.; Raines, R. T. Bright building blocks for chemical biology. *ACS Chem. Biol.* **2014**, *9*, 855−866.
(67) Grimm, J. B.; English, B. P.; Chen, J.; Slaughter, J. P.; Zhang, Z.; Revyakin, A.; Patel, R.; Macklin, J. J.; Normanno, D.; Singer, R. H.; Lionnet, T.; Lavis, L. D. A general method to improve fluorophores for live-cell and single-molecule microscopy. *Nat. Methods* **2015**, *12*, 244−250.
(68) Zhou, X.; Lai, R.; Beck, J. R.; Li, H.; Stains, C. I. Nebraska Red: A phosphinate-based near-infrared fluorophore scaffold for chemical biology applications. *Chem. Commun.* **2016**, *52*, 12290−12293.
(69) Grimm, J. B.; Muthusamy, A. K.; Liang, Y.; Brown, T. A.; Lemon, W. C.; Patel, R.; Lu, R.; Macklin, J. J.; Keller, P. J.; Ji, N.; Lavis, L. D. A general method to fine-tune fluorophores for live-cell and in vivo imaging. *Nat. Methods* **2017**, *14*, 987−994.
(70) Zhou, X.; Lesiak, L.; Lai, R.; Beck, J. R.; Zhao, J.; Elowsky, C. G.; Li, H.; Stains, C. I. Chemoselective alteration of fluorophore scaffolds as a strategy for the development of ratiometric chemodosimeters. *Angew. Chem., Int. Ed.* **2017**, *56*, 4197−4200.
(71) Fang, Y.; Good, G. N.; Zhou, X.; Stains, C. I. Phosphinate-containing rhodol and fluorescein scaffolds for the development of bioprobes. *Chem. Commun.* **2019**, *55*, 5962−5965.
(72) Brøndsted, F.; Stains, C. I. Heteroatom-substituted xanthene fluorophores enter the shortwave-infrared region. *Photochem. Photobiol.* **2022**, *98*, 400−403.
(73) Brøndsted, F.; Fang, Y.; Li, L.; Zhou, X.; Grant, S.; Stains, C. I. Single atom stabilization of phosphinate ester-containing rhodamines yields cell permeable probes for turn-on photoacoustic imaging. *Chem. −Eur. J.* **2024**, *30* (1), No. e202303038, DOI: 10.1002/chem.202303038.
(74) Lavis, L. D.; Rutkoski, T. J.; Raines, R. T. Tuning the pK_a of fluorescein to optimize binding assays. *Anal. Chem.* **2007**, *79*, 6775−6782.
(75) Grimm, J. B.; Gruber, T. D.; Ortiz, G.; Brown, T. A.; Lavis, L. D. Virginia Orange: A versatile, red-shifted fluorescein scaffold for single- and dual-input fluorogenic probes. *Bioconjugate Chem.* **2016**, *27*, 474−480.
(76) Martineau, M.; Somasundaram, A.; Grimm, J. B.; Gruber, T. D.; Choquet, D.; Taraska, J. W.; Lavis, L. D.; Perrais, D. Semisynthetic fluorescent pH sensors for imaging exocytosis and endocytosis. *Nat. Commun.* **2017**, *8*, No. 1412.
(77) Hu, Y.-B.; Dammer, E. B.; Ren, R.-J.; Wang, G. The endosomal−lysosomal system: From acidification and cargo sorting to neurodegeneration. *Transl. Neurodegener.* **2015**, *4*, 18 DOI: 10.1186/s40035-015-0041-1.
(78) Cheah, K. M.; Jun, J. V.; Wittrup, K. D.; Raines, R. T. Host−guest complexation by β-cyclodextrin enhances the solubility of an esterified protein. *Mol. Pharmaceutics* **2022**, *19*, 3869−3876.
(79) Deprey, K.; Kritzer, J. A. HaloTag forms an intramolecular disulfide. *Bioconjugate Chem.* **2021**, *32*, 964−970.
(80) Akishiba, M.; Futaki, S. Inducible membrane permeabilization by attenuated lytic peptides: A new concept for accessing cell interiors through ruffled membranes. *Mol. Pharmaceutics* **2019**, *16*, 2540−2548.
(81) Nomura, Y.; Sakamoto, K.; Akishiba, M.; Iwata, T.; Hirose, H.; Futaki, S. Improved cytosolic delivery of macromolecules through dimerization of attenuated lytic peptides. *Bioorg. Med. Chem. Lett.* **2020**, *30*, No. 127362.
(82) Becker, B.; Englert, S.; Schneider, H.; Yanakieva, D.; Hofmann, S.; Dombrowsky, C.; Macarrón Palacios, A.; Bitsch, S.; Elter, A.; Meckel, T.; Kugler, B.; Schirmacher, A.; Avrutina, O.; Diederichsen, U.; Kolmar, H. Multivalent dextran hybrids for efficient cytosolic delivery of biomolecular cargoes. *J. Pept. Sci.* **2021**, *27*, e3298.
(83) Feng, R.; Ni, R.; Chau, Y. Fusogenic peptide modification to enhance gene delivery by peptide−DNA nano-coassemblies. *Biomat. Sci.* **2022**, *10*, 5116−5120.

https://doi.org/10.1021/acschembio.3c00713
ACS Chem. Biol. 2024, 19, 908−915